

1 **THE ESSENTIAL KINASE TgGSK REGULATES CENTROSOME DIVISION AND ENDODYOGENY IN**
2 ***TOXOPLASMA GONDII***

3 Amanda Krueger¹, Sofia Horjales², Chunlin Yang¹, William J. Blakely¹, Maria E. Francia²,
4 Gustavo Arrizabalaga^{1,3#}

5 ¹*Department of Pharmacology and Toxicology, Indiana University School of Medicine*

6 ²*Laboratory of Apicomplexan Biology, Institut Pasteur de Montevideo*

7 ³*Department of Microbiology and Immunology, Jacobs School of Medicine and*
8 *Biomedical Sciences, University at Buffalo*

9 #Corresponding author

10 Address: 955 Main Street, Room 6155

11 Buffalo, NY, 14203

12 Email: garrizab@buffalo.edu

13 Short title: Characterization of *Toxoplasma gondii* GSK

14 **ABSTRACT**

15 Intracellular replication is crucial for the success of apicomplexan parasites, including
16 *Toxoplasma gondii*. Therefore, essential players in parasite replication present potential
17 targets for drug development. In this study, we have characterized TgGSK, a glycogen
18 synthase kinase homolog that plays an important role in *Toxoplasma* endodyogeny. We
19 have shown that TgGSK has a dynamic localization that is concurrent with the cell cycle.
20 In non-dividing parasites, this kinase is highly concentrated in the nucleus. However,
21 during division, TgGSK displays a cytosolic localization, with concentration foci at the
22 centrosomes, a key organelle involved in parasite division, and the basal end. Conditional
23 knockdown of TgGSK determined that it is essential for the completion of the lytic cycle
24 and proper parasite division. Parasites lacking endogenous protein levels of TgGSK
25 exhibited defects in division synchronicity and the segregation of the nucleus and
26 apicoplast into forming daughter cells. These phenotypes are associated with defects in
27 centrosome duplication and fission. Global phosphoproteomic analysis determined
28 TgGSK-dependent phosphorylation of RNA-processing, basal end, and centrosome
29 proteins. Consistent with the putative regulation of RNA-processing proteins, global
30 transcriptomic analysis suggests that TgGSK is needed for proper splicing. Finally, we
31 show that TgGSK interacts with GCN5b, a well-characterized acetyltransferase with roles
32 in transcriptional control. Conversely, GCN5b chemical inhibition results in specific
33 degradation of TgGSK. Thus, these studies reveal the involvement of TgGSK in various
34 crucial processes, including endodyogeny and splicing, and identify acetylation as a
35 possible mechanism by which this essential kinase is regulated.

36

37 **AUTHOR SUMMARY**

38 *Toxoplasma gondii* infects nearly a third of the world's human population. While
39 infection is largely asymptomatic in healthy adults, in immunocompromised or
40 immunosuppressed individuals it can lead to brain lesions and even death. Similarly,
41 toxoplasmosis can result in stillbirth, birth defects, and blindness of a developing fetus in
42 the case of a congenital infection. With minimal treatments for Toxoplasmosis available,
43 it is crucial to study parasite-specific processes that could be potential drug targets for the
44 treatment of Toxoplasmosis. In this study, we investigated the protein TgGSK that is
45 essential for parasite survival and proper division. We showed that TgGSK may perform
46 its essential functions through interaction with the centrosome, an organelle that plays a
47 major role in cell division in many organisms. We also show in this study a role for TgGSK
48 in proper processing of messenger RNAs. Taken together, we have performed an in-depth
49 study of the functional role of the essential protein TgGSK in *Toxoplasma gondii*.
50 Importantly, TgGSK was shown to have more similarity to plant proteins than mammalian
51 proteins which may allow for the possibility of targeting of this protein for therapeutic
52 treatment of toxoplasmosis.

53 INTRODUCTION

54 *Toxoplasma gondii* is an obligate intracellular parasite that infects approximately a
55 third of the world's human population [1]. The parasite's ability to be highly symptomatic
56 in those immunocompromised or infected congenitally makes *Toxoplasma* a globally
57 relevant pathogen [2,3]. Many of the negative effects of an uncontrolled *Toxoplasma*
58 infection are a consequence of the lytic cycle of the highly replicative tachyzoite form,
59 which is responsible for the acute stage of the disease. Tachyzoites actively invade any
60 nucleated cell forming a parasitophorous vacuole in the process. After several rounds of
61 asexual division within this vacuole, the parasite actively exits, lysing the parasitophorous
62 vacuole and host cell in the process. Once outside the cell, the parasite quickly invades
63 neighboring cells, allowing for propagation and continuation of the acute stage of the
64 infection.

65 Intracellular division of *Toxoplasma* occurs by the divergent process of endodyogeny,
66 through which two daughter parasites gradually form within a mature mother [4,5]. The
67 assembly of daughter cells is supported by the inner membrane complex (IMC), which
68 consists of a series of flattened membrane vesicles stitched together and that, along with
69 the parasite's plasmalemma, forms the so-called pellicle. Underneath the pellicle and
70 serving a role in parasite shape and polarity are a set of 22 subpellicular microtubules.
71 Early in endodyogeny, IMCs for each of the daughter cells emanate within the mother
72 cell. Another early event in parasite division is the duplication of the centrosome, which,
73 in addition to serving conserved roles across eukaryotes in nuclear mitosis, acts as an
74 organizing center for subpellicular microtubules as well as serving as a contact site for
75 various other dividing organelles in *Toxoplasma* [6]. As the IMCs of the two daughter cells

76 grow, some organelles are made *de novo*, while the nucleus, the mitochondrion, and the
77 plastid-like apicoplast divide between them. The IMC of the mother eventually disappears
78 as the two nascent parasites occupy the bulk of the mother parasite. Finally, the original
79 plasmalemma envelopes the two new cells, and a cleavage furrow extends between the
80 daughters. The various steps that make up endodyogeny have been well described.
81 Nonetheless, the signals and regulatory proteins controlling endodyogeny and the
82 stepwise structural assembly of the cytoskeletal elements are not well understood.

83 Recently, we characterized the plant-like phosphatase PPKL, which regulates
84 daughter cell formation in *Toxoplasma* [7]. PPKL is essential for parasite propagation, and
85 lack of PPKL uncouples DNA duplication, which occurs normally in PPKL knockdown
86 parasites, from daughter cell formation [7]. Knockdown of PPKL also affects the rigidity
87 and organization of cortical microtubules, although it does not affect centrosome
88 duplication. Interestingly, the phosphorylation of the known cell cycle regulator CRK1 is
89 altered in PPKL knockdown parasites, suggesting that PPKL regulates parasite division
90 by impacting the CRK-1-dependent signaling pathway [7]. PPKL is homologous to the
91 *Arabidopsis* phosphatase BSU1, which is at the center of the plant brassinosteroid
92 pathway [8,9]. In the absence of brassinosteroid, the phosphorylated kinase BIN2
93 inactivates transcription factors that regulate the expression of genes involved in various
94 processes, including plant tissue growth, development, and stress responses.
95 Brassinosteroid activates a cascade that results in the activation of BSU1, which in turn
96 dephosphorylates BIN2 at a conserved tyrosine, inactivating it and leading to the
97 transcription of brassinosteroid response genes. *Toxoplasma* does not produce
98 brassinosteroid, and a search for other members of this well-characterized plant signaling

99 pathway did not reveal clear homologs except for TGGT1_265330, which shows strong
100 similarity to BIN2. As BIN2 from plants are members of the family of glycogen synthase
101 kinase 3 (GSK3) serine/threonine kinases, we refer to TGGT1_265330 as TgGSK. A
102 previous study, which referred to this protein as TPK3, indicated that it bears 54%
103 homology to GSKs over the catalytic domain and showed that the recombinant protein
104 has kinase activity and can autophosphorylate [10]. Nonetheless, the localization or
105 function of this *Toxoplasma* kinase was not investigated.

106 Here, we report an in-depth analysis of TgGSK. We show that TgGSK is an essential
107 kinase in *Toxoplasma* that displays a varying localization dependent on parasite division.
108 Knockdown of TgGSK causes abnormal division phenotypes, including defects in the
109 centrosome, apicoplast, and nuclear segregation. Furthermore, phosphoproteome and
110 transcriptome analyses suggest a role in splicing for TgGSK. Finally, we show that TgGSK
111 forms a complex with the acetyltransferase GCN5b and that inhibition of GCN5b
112 acetyltransferase activity leads to TgGSK degradation. In sum, our work characterizes an
113 essential kinase that regulates a variety of critical functions in the human pathogen
114 *Toxoplasma gondii*, uncovering a potential target for therapeutic intervention.

115 RESULTS

116 TOXOPLASMA GSK IS RELATED TO PLANT KINASES

117 Previously, we characterized the Kelch domain-containing protein phosphatase
118 PPKL in *Toxoplasma gondii* [7]. *Toxoplasma* PPKL is a homolog of the plant
119 phosphatase BSU1, which is central to the brassinosteroid signaling pathway [8,9].
120 *Toxoplasma* does not produce brassinosteroid, and a search for other members of this
121 well-characterized plant signaling pathway did not reveal clear homologs except for
122 TGGT1_265330, which shows 53% identity to the PPKL substrate BIN2. BIN2 from
123 plants are members of the family of glycogen synthase kinase 3 (GSK3)
124 serine/threonine kinases. Thus, though this kinase had been previously referred to as
125 TPK3 (*Toxoplasma* Protein Kinase 3), we here rename the product of TGGT1_265330
126 as TgGSK to better reflect its evolutionary origin and putative function. This protein is
127 a 394 amino acid conventional kinase with an ATP binding site and an active site and
128 shows homology to members of the GSK family of kinases. GSKs are unique among
129 eukaryotic protein kinases (ePKs) in that they have a cluster of conserved amino acids
130 that might perform a regulatory role. In mammalian GSK3 β , these correspond to
131 residues Q89, R92, F93, K94, and N95 [11]. TgGSK contains this cluster between
132 amino acids 80 and 87. Moreover, existing phosphoproteomic data [12] shows that
133 TgGSK is phosphorylated at four serine/threonine sites (T38, S208, S210, and S270)
134 and at one tyrosine (Y211), which is conserved throughout the GSK family (**Fig 1A**).
135 The amino acids surrounding the conserved tyrosine site are conserved across all
136 GSKs, including in Apicomplexa, plants, and mammals (**Fig 1B**). A clustal omega
137 alignment of TgGSK along with GSK homologs from the malarial parasite *Plasmodium*,

138 humans, and *Arabidopsis*, shows that TgGSK and *Plasmodium* GSK cluster with the
139 *Arabidopsis thaliana* BIN2 (**Fig. 1C**). Thus, it appears that TgGSK has greater
140 homology to plant BIN2 than to mammalian GSK3.

141 **TGGSK HAS A DYNAMIC LOCALIZATION THAT IS CELL CYCLE DEPENDENT**

142 To determine the localization of TgGSK within the parasite, we used CRISPR/Cas9 to
143 generate a strain in which the endogenous protein includes a triple hemagglutinin (3xHA)
144 epitope tag in its carboxy terminus. Western blot analysis of the resulting strain,
145 $\Delta Ku80$:TgGSK.3xHA (from here on referred to as GSK.3xHA), shows a protein of
146 approximately 44 kDa, which matches the expected molecular weight of TgGSK (**Fig.**
147 **2A**). Using this validated strain, we performed immunofluorescence assays (IFA) of
148 intracellular parasites probing for HA to observe TgGSK and for IMC3 to monitor the inner
149 membrane complex (IMC) (**Fig. 2B**). IMC3 is present in both mother and daughter
150 parasites, which allows us to differentiate between dividing (those with daughter parasites
151 within) and non-dividing (those without daughter parasites) parasites. Interestingly, we
152 noted that while in non-dividing parasites, TgGSK is more concentrated in the nucleus, in
153 those undergoing division TgGSK is evenly distributed throughout the entire cell (**Fig.**
154 **2B**). To explore this dynamic localization, we monitored TgGSK's localization in parasites
155 at various stages of division (**Fig. 2C**). Throughout all stages of division, we saw TgGSK
156 distributed throughout the cell, while in non-dividing parasites TgGSK consistently
157 localized to the nucleus. While the difference in GSK localization in dividing and non-
158 dividing parasites is evident, we aimed to quantify this observation. For this purpose, we
159 imaged 20 non-dividing parasites and 20 parasites in the late division stage and used
160 ImageJ to quantify the fluorescent intensity of the HA signal in the cytosol and the nucleus.

161 As expected, this analysis determined a higher ratio of nuclear over cytosolic signal in
162 non-dividing parasites (**Fig. 2D**).

163 To obtain a more detailed understanding of TgGSK's localization, we performed
164 ultrastructure expansion microscopy (UExM), which allows for higher-resolution analysis.
165 As with standard IFA, we detect TgGSK within the nucleus. Interestingly, we also detect
166 TgGSK in areas of tubulin concentration, which are reminiscent of centrosomes, as well
167 as in the basal end of the parasites (**Fig. 2E**). Given the apparent localization of TgGSK
168 to the centrosome, we co-stained for TgGSK and Centrin 1. Indeed, TgGSK and Centrin
169 1 appear to localize to the same area, confirming TgGSK's concentration around the
170 centrosomes in both non-dividing and dividing parasites (**Fig. 2F**). In sum, IFA and UExM
171 analyses show that TgGSK has a dynamic localization dependent on the division stage
172 and is present at the centrosomes, suggesting that TgGSK may play a role in the
173 regulation of parasite replication.

174 **TgGSK IS ESSENTIAL FOR PARASITE SURVIVAL**

175 In a *Toxoplasma* genome-wide CRISPR screen, TgGSK was assigned a fitness value
176 of -4.12 [13], which suggests that this protein is essential and, therefore, a full knockout
177 would likely not be possible. Accordingly, we used a conditional knockdown approach to
178 investigate the function of TgGSK. For this purpose, we replaced the TgGSK promoter
179 with the tetracycline regulatable promoter (TATi) [14] in the GSK.3xHA strain using
180 CRISPR/Cas9 (**Fig. 3A**). IFA showed that TgGSK's localization is unchanged in the
181 resulting strain (TATi-GSK.3xHA) (**Fig. 3B**). Importantly, western blot analysis shows that
182 TgGSK expression is significantly reduced after 42 hours of treatment with the
183 tetracycline analog aTC, with near complete lack of protein at 72 hours (**Fig. 3C**). To

184 determine if TgGSK is required for parasite propagation, we performed a plaque assay
185 with the parental and the TATi-GSK.3xHA strains with and without aTC. Consistent with
186 the results of the CRISPR screen, TATi-GSK.3xHA parasites grown in the presence of
187 aTC failed to form plaques (**Fig. 3D and E**), indicating that TgGSK is essential for parasite
188 survival and propagation.

189 **KNOCKDOWN OF TgGSK CAUSES ABNORMAL DIVISION PHENOTYPES**

190 To explore the impact of TgGSK's loss on cell division, we performed IFAs on the TATi-
191 GSK.3xHA strain grown with and without aTC. Staining for IMC3 reveals significant
192 division defects after 42 hours of aTC treatment, at which time point there is still some
193 TgGSK present, albeit at reduced levels (**Fig. 4A**). The most common phenotypes
194 observed include asynchronous division, incomplete nuclear segregation, and vacuoles
195 with parasites of abnormal shape (**Fig. 4A**). Quantification of 100 vacuoles over three
196 experimental replicates showed that, while $76.5\% \pm 2.2\%$ of parasites appear to divide
197 normally in the absence of aTC, only $22.9\% \pm 3.18\%$ of parasites exhibit normal division in
198 the presence of aTC (**Fig. 4B**). Among the vacuoles grown with aTC that show aberrant
199 division, $51.9\% \pm 1.5\%$ exhibit asynchronous division, $28.6\% \pm 2.4\%$ uneven segregation,
200 and $19.4\% \pm 2.9\%$ abnormally shaped parasites (**Fig. 4C**). When parasites were allowed
201 to grow in aTC for 96 hours, there was an exacerbation of all phenotypes as the parasites
202 appear to continue dividing unsuccessfully (**Fig. 4D**). Notably, significant defects are seen
203 in parasite structure, with acetylated tubulin not being organized adequately into individual
204 fully closed parasites, and in nuclear segregation. Interestingly, there also seems to be a
205 defect in chromatin condensation, as shown by diffuse staining for the histone marker H2

206 **(Fig. 4D)**. Overall, analysis of the TgGSK knockdown strain reveals a function for this
207 kinase in parasite division.

208 **TgGSK KNOCKDOWN CAUSES CENTROSOME ABNORMALITIES**

209 Since we detected TgGSK in the centrosomes and observed nuclear segregation
210 defects in TgGSK knockdown parasites, we asked if knockdown also caused centrosome
211 abnormalities. Indeed, using IFA staining for Centrin 1 and the mitotic spindle marker EB1,
212 we detect abnormalities in centrosome morphology upon TgGSK knockdown **(Fig. 5A)**.
213 Specifically, we observe elongated centrosomes and some that seem unable to undergo
214 fission. We quantified the distribution of EB1 and centrin per parasite nucleus from our
215 IFA images using ImageJ. In a normal parasite culture, where around 30% of parasites
216 are dividing, the average amount of centrosomes per nucleus should be around 1.25, with
217 non-dividing parasites having one centrosome and dividing parasites having two [13].
218 EB1 recruitment to the mitotic spindle accompanies centrosome duplication and is only
219 detectable in dividing parasites. While there was no significant difference in the number
220 of nuclei displaying EB1 foci between control and TgGSK knockdown parasites, there
221 was a significant difference in the number of centrosomes associated with each parasite
222 nucleus **(Fig. 5B)**. The aTC-treated parasites had a lower average number of
223 centrosomes per nucleus, with some vacuoles displaying only one centrosome for four
224 parasite nuclei **(Fig. 5B)**. Importantly, UExM confirmed the various phenotypes observed
225 by IFA (e.g. abnormal parasite structure and nuclear segregation defects) and highlighted
226 the abnormally shaped centrosomes at a higher resolution **(Fig. 5C)**. Given the
227 centrosome's key role in parasite division and organellar segregation, the various

228 division-related phenotypes observed in the TgGSK knockdown parasites might be a
229 consequence of the centrosome segregation defects present in the mutant.

230 **KNOCKDOWN OF TgGSK AFFECTS APICOPLAST DIVISION**

231 It is known that the centrosomes also coordinate the segregation of other organelles,
232 including the apicoplast [15]. Accordingly, we monitored apicoplast division and
233 segregation by monitoring the apicoplast marker CPN60 (**Fig. 6A**). While parasites grown
234 in the absence of aTC averaged around one apicoplast per parasite nucleus, aTC treated
235 parasites averaged one apicoplast for every four parasite nuclei (**Fig. 6B**). Therefore, it
236 appears that, in addition to abnormal nuclear division and segregation, apicoplast division
237 and segregation are also disrupted in TgGSK knockdown parasites.

238 **CENTROSOMAL, BASAL END, AND SPLICING PROTEINS SHOW TgGSK-DEPENDENT** 239 **PHOSPHORYLATION**

240 Since TgGSK has the structure of a conventional kinase and is a member of the GSK
241 family, we performed global phosphoproteome analysis to determine proteins that have
242 TgGSK-dependent phosphorylation. We found 27 proteins with peptides that had
243 decreased phosphorylation and 40 proteins with peptides that had increased
244 phosphorylation in TgGSK knockdown parasites compared to parental ($\text{Log}_2\text{FC} > 0.5$,
245 $p < 0.05$) (**Fig. 7A and supplemental dataset 1**). Using ToxoDB and StringDB, we
246 identified a few enriched pathways involving some of the 67 proteins displaying TgGSK-
247 dependent phosphorylation. Three of the 27 proteins that had decreased phosphorylation
248 in the knockdown were RNA-binding or known splicing proteins (**Fig. 7B**). Another three
249 proteins with decreased phosphorylation were members of the MyoC glideosome
250 complex in the basal end of the parasite (**Fig. 7B**). Interestingly, of these six proteins of

251 interest, five of them were differentially phosphorylated at an S/TXXXS/T motif, typical of
252 GSK substrates [16]. In addition to splicing and basal end proteins, the protein that had
253 the highest increase in phosphorylation in the knockdown was Centrin 2 (**Fig. 7B**). In
254 addition, analysis of the hypothetical proteins with TgGSK-dependent phosphorylation
255 revealed that 18% of those could be involved in RNA metabolism (**Supplemental figure**
256 **1**). Overall, phosphoproteome analysis suggests that TgGSK might influence the
257 regulation of proteins related to the centrosomes, basal complex, and splicing.

258 **TgGSK INTERACTS AND IS REGULATED BY THE GCN5B COMPLEX**

259 To further understand the role of TgGSK and the phenotypes associated with its loss,
260 we performed immunoprecipitation followed by mass spectrometry to identify putative
261 interacting partners. Interestingly, the top nine significant TgGSK interacting proteins were
262 all in the nucleus, with eight of them being members of the GCN5b complex (**Table 1 and**
263 **supplemental dataset 2**). The GCN5b complex is present in the nucleus, where it
264 acetylates histones to open chromatin for gene transcription [17].

265 While it is plausible that TgGSK regulates members of the GCN5b complex via
266 phosphorylation, we did not identify any of them as part of the TgGSK-dependent
267 phosphoproteome. Accordingly, we explored whether, alternatively, the GCN5b complex
268 might regulate TgGSK. For this purpose, we treated parasites with Garcinol, an
269 acetyltransferase inhibitor that has been shown to specifically inhibit the histone
270 acetylation activity of GCN5b in *Toxoplasma* [18]. We treated GSK.3xHA parasites with
271 0, 2, or 4 μ M of Garcinol overnight and monitored TgGSK localization by IFA. Interestingly,
272 we found that while there was no difference in TgGSK localization pattern after this
273 incubation time, the overall TgGSK signal was reduced in a Garcinol dose-dependent

274 manner, with the signal being absent after treatment with 4 μ M of Garcinol (**Fig. 8A**). To
275 confirm these results, we performed western blot analysis using the same Garcinol
276 concentrations. We saw a reduction in TgGSK protein levels after treatment with 2 μ M of
277 Garcinol and a complete absence of protein after treatment with 4 μ M of Garcinol (**Fig.**
278 **8B**). As a control, we also stained for aldolase, which did not seem to be affected across
279 all Garcinol concentrations tested (**Fig. 8B**). Interestingly, previously published data
280 showed that TgGSK expression level was not changed by Garcinol treatment, further
281 suggesting that TgGSK is regulated by GCN5b at the protein level [18]. Therefore, it
282 appears that TgGSK's protein expression or stability might be regulated by GCN5b.

283 **TgGSK KNOCKDOWN CAUSES DIFFERENTIAL TRANSCRIPTION AND SPLICING**

284 As we detected TgGSK in the nucleus and determined that it is in a complex with
285 transcription factors we investigated the effect of TgGSK knockdown on global
286 transcription. For this purpose, we performed RNAseq of the TATi-GSK.3xHA strain grown
287 for 18 hours with or without aTC. We used 18 hours, at which time point there is still
288 TgGSK protein, to avoid transcript changes associated with parasite death. We found that
289 there were 405 genes downregulated and 157 genes upregulated when TgGSK was
290 knocked down (Log₂FC>0.5, p<0.05) (**Fig. 9A and supplemental dataset 3**). The
291 differentially regulated genes were members of many different pathways, with most of
292 them being either hypothetical or not falling into any enriched pathway (**Fig. 9B**).
293 Comparison of the dysregulated genes with those whose promoters are known to be
294 bound by the GCN5b complex did not reveal any enrichment for GCN5b regulated genes
295 [17].

296 As we identified several RNA processing proteins that had TgGSK-dependent
297 phosphorylation, we investigated the RNAseq data for splicing variants. Interestingly, we
298 found that 131 genes had exon differences in TgGSK knockdown parasites compared to
299 parental (**Fig. 9C**). Since this data was taken at 18 hours of aTC treatment, we infer that
300 these splicing differences were not due to parasite death. However, as an additional
301 control, we also analyzed exon differences in the transcriptome of the TgPPKL
302 knockdown parasites, which, like TgGSK, is essential, and its disruption causes division-
303 related defects [7]. We found that compared to parental, only five genes were differentially
304 spliced (**Fig. 9C**). In addition, since the garcinol treatment resulted in loss of TgGSK, we
305 mined previously published transcriptomic data from garcinol-treated parasites [18] to
306 assess the effects on splicing. This analysis revealed 149 differentially spliced transcripts
307 in parasites treated with 4 μ M Garcinol (**Fig. 9C**). Interestingly, 24 of these overlapped
308 with transcripts that were differentially spliced in the TgGSK knockdown (**Fig. 9C**).
309 Overall, these data suggest that TgGSK plays a role in proper splicing and this effect is
310 seen after both TgGSK transcriptional knockdown and protein degradation.

311 **DISCUSSION**

312 Members of the glycogen synthase kinase (GSK) protein family are serine/threonine
313 kinases present in many organisms, including mammals and plants [19]. Most
314 mammalian species encode for two GSKs, GSK3 α and GSK3 β , with hundreds of
315 substrates that play roles in cellular proliferation and migration, glucose regulation, and
316 apoptosis [20]. By contrast, most plant species encode 10 GSKs, which fall into four major
317 groups and are involved in plant growth, development, and stress response [21]. All GSKs
318 have a single conserved tyrosine residue that can be phosphorylated [22]. This residue

319 has been shown to interact in the binding pocket to control kinase regulation [23]. In
320 Arabidopsis, this tyrosine is dephosphorylated by the protein phosphatase BSU1, leading
321 to its inactivation [9]. Interestingly, *Toxoplasma gondii*, like other parasites of the phylum
322 Apicomplexa, encode for two putative GSKs (TGGT1_265330 and TGGT1_266910),
323 which are, by and large, uncharacterized. In the current study, we investigated the
324 localization and function of TGGT1_265330, which we refer to as TgGSK. We found that
325 TgGSK localization is dependent on the cell cycle and that depletion of TgGSK impacts
326 parasite daughter formation, nuclear segregation, centrosome dynamics and fission, and
327 apicoplast dynamics. Our findings also demonstrated that TgGSK might play a role in the
328 regulation of splicing and that its stability is dependent on the GCN5b lysine
329 acetyltransferase.

330 The asexual division of *Toxoplasma* occurs by the unusual process of endodyogeny,
331 which is defined by the gradual formation of two daughter parasites within a mature one.
332 The centrosome is an essential component of this division process, with each daughter
333 parasite forming around a centrosome, which undergoes fission in early S phase [25].
334 The centrosome has been shown to nucleate spindle microtubules during mitosis [25].
335 Later, during cytokinesis, the centrosome organizes the scaffolding of daughter cell
336 components to allow for nuclear fission and correct organelle segregation into daughter
337 parasites [25]. One of the organelles that is associated with the centrosomes during
338 division is the apicoplast, a non-photosynthetic plastid organelle [15]. Before apicoplast
339 fission, the organelle elongates, with each end interacting with a centrosome. Therefore,
340 the centrosomes act to correctly orient the apicoplast to allow for proper fission. By UExM,
341 we were able to visualize TgGSK at the centrosomes. In addition, knockdown of TgGSK

342 led to defects in centrosome number, with not every parasite nucleus having an
343 associated centrosome. We also observed defects in centrosome duplication, with
344 centrosomes that appeared to be duplicated but unable to undergo fission. These
345 centrosome abnormalities could underlie the other division phenotypes we observe, such
346 as nuclear and apicoplast segregation defects. Interestingly, we also observed TgGSK-
347 dependent phosphorylation of Centrin 2, a protein that is localized to the centrosomes
348 and has been shown to be essential for parasite division and correct centrosome
349 segregation [26]. In our study, Centrin 2 phosphorylation was increased during TgGSK
350 knockdown, suggesting that it is not a TgGSK substrate and that its regulation of Centrin
351 2 is indirect. Interestingly, Centrin 2 has also been shown to be localized to the basal body
352 [26]. As we also detect TgGSK within the basal end of the parasite, it is unclear whether
353 the functional relationship between these two proteins occurs at the centrosome or in the
354 basal body.

355 A role for GSKs in centrosome regulation is also observed in other organisms. For
356 example, inhibition of GSK3 β in human cancer cells results in centrosome dysregulation
357 and abnormal mitosis [27]. Similarly, in HeLa cells, GSK3 β plays a role in the organization
358 of microtubule arrays derived from the centrosomes [28]. The knockdown of GSK3 β
359 reduced the amount of centrosomally focused microtubules and caused the
360 mislocalization of various centrosomal proteins [28]. Though recruitment of the mitotic
361 spindle binding protein EB1 is not altered in the absence of TgGSK, further studies would
362 need to be done in *Toxoplasma* to determine if centrosomal proteins or mitotic factors are
363 negatively affected in the absence of TgGSK.

364 Intriguingly, we determined that the phosphorylation state of three RNA-binding
365 proteins (TGGT1_264610, TGGT1_275480, and TGGT1_304630) are altered in the
366 absence of TgGSK. While TGGT1_264610 and TGGT1_304630 are characterized as
367 putative RNA binding proteins in *Toxoplasma*, StringDB analysis characterized them as
368 proteins related to splicing. TGGT1_275480 is homologous to the pre-splicing factor
369 CEF1. Interestingly, all three of these proteins contain the S/TXXXS/T motif, suggesting
370 that they may be direct substrates of TgGSK [17]. As with GSKs in the centrosomes, there
371 is evidence from other organisms highlighting the potential role GSKs play in splicing. A
372 study in mouse embryonic stem cells found that inhibition of GSK3 altered the splicing of
373 188 mRNAs [29]. GSK was also shown to interact with multiple SR family splicing proteins
374 and various other RNA-binding proteins [29]. In human T-cells, phosphorylation of the
375 nuclear RNA biogenesis protein PSF by GSK3 controls the alternative splicing of CD45
376 [30]. While there is no direct evidence for a role in splicing for the plant GSK homolog
377 BIN2, mapping of the BIN2 signaling network identified 13 RNA processing proteins [31].
378 Thus, it is plausible that *Toxoplasma* TgGSK directly or indirectly regulates the function
379 of RNA processing proteins. Consistent with this idea, we observed an increase in
380 alternatively spliced transcripts upon knockdown of TgGSK.

381 One of the most intriguing findings of our studies is the possible regulation of TgGSK
382 by the lysine acetyltransferase GCN5b. We observed that TgGSK interacts with a well-
383 characterized GCN5b-containing complex. *Toxoplasma* encodes for two GCN5 proteins,
384 with GCN5b being essential for parasite viability [17]. The GCN5b complex is in the
385 nucleus, where it performs its primary function of acetylating histones [17]. GCN5b has
386 been shown to be present in a complex that includes the ADA2a adaptor protein and

387 various plant-like AP2 transcription factors [32]. There appear to be two distinct stable
388 GCN5b-containing complexes in *Toxoplasma*, one which includes the putative
389 transcription factors AP2X8 and AP2IX7 and the other which includes AP2XII4 and
390 AP2VIIa5 [32]. Our results indicate that TgGSK interacts with the complex that includes
391 AP2X8 and AP2IX7 (**Table 1**). Interestingly, previous characterization of the *Toxoplasma*
392 GCN5b complexes identified TgGSK as an interactor, which validates the interaction
393 between TgGSK and this complex [32].

394 Not only did we detect a physical interaction between TgGSK and the GCN5b
395 complex, but we also observed a specific loss of TgGSK upon GCN5b inhibition by
396 Garcinol. These results bring up the possibility that GCN5b regulates TgGSK via
397 acetylation. While acetylation of histones is canonical for histone acetyltransferases, there
398 have been many studies showing acetylation of non-histone proteins in various organisms
399 [33,34]. Non-histone protein acetylation has been found to play a broad diversity of roles,
400 including protein folding and stability [35]. Consistent with a possible role of acetylation in
401 the regulation of TgGSK, a global acetylome study in *Toxoplasma* identified lysine
402 acetylation on TgGSK at residue K13 in extracellular parasites. Intriguingly, a whole
403 proteome mapping of ubiquitination showed that K13 is also ubiquitinated [36]. Cross-talk
404 between acetylation and ubiquitination of the same lysine is well known and is of particular
405 importance in the context of protein stability, where lysine acetylation can block
406 proteasome-mediated degradation by lysine acetylation [37]. Thus, our data points to a
407 novel mechanism of TgGSK regulation via the competition between acetylation and
408 ubiquitination (**Fig. 10**). We propose that TgGSK regulation could involve its acetylation
409 within the nucleus by GCN5b at residue K13 before being trafficked to the cytosol and

410 centrosomes in preparation for cell division. Once division has finished, TgGSK could be
411 deacetylated and ubiquitinated at K13, causing its degradation (**Fig. 10**). Further studies
412 focused on whether K13 in TgGSK plays a direct role in the stability and function of the
413 protein are thus warranted as it would elucidate a novel mechanism of GSK regulation.

414 While phosphorylation in the activation loop is the best understood mechanism by
415 which GSKs are regulated, a role for acetylation has also been reported. For example,
416 mammalian GSK3 β is acetylated at residue K183, and this acetylation is involved in
417 kinase regulation [38]. A study of GSK3 β in Alzheimer's disease found that acetylation of
418 GSK3 β at residue K15 (the equivalent of TgGSK K13) led to the over-activation of the
419 kinase, which led to the promotion of tau hyperphosphorylation and an increase in
420 disease phenotypes [39]. In plants, HDAC6 removes acetylation on the GSK homolog
421 BIN2 at residue K186 to inhibit kinase activity and enhance brassinosteroid signaling [40].
422 That study also showed that the acetylation and phosphorylation sites are both in the
423 binding pocket and interact to regulate the kinase activity of BIN2 [40]. Interestingly, the
424 residue shown to be acetylated in plants and mammals (K186 and K183, respectively) is
425 conserved in *Toxoplasma*, but the acetylome data does not show that this residue is
426 modified [41].

427 Overall, the findings in this study highlight the various roles of TgGSK in *Toxoplasma*.
428 As BIN2 and mammalian GSKs have been shown to have hundreds of substrates with
429 many different biological functions, the broad range of possible TgGSK functions
430 uncovered here is not surprising. While likely roles for TgGSK in the centrosome and
431 splicing have been identified through this work, further studies are warranted to
432 understand the mechanistic underpinning of these functions. The critical importance of

433 this essential kinase underscores its strong potential as a target for antiparasitic
434 intervention.
435

436 **MATERIALS AND METHODS**

437 **Parasite strains and reagents**

438 All parasite strains used in this study derived from the strain RH lacking HXGPRT and
439 Ku80 (RH $\Delta ku80\Delta hxgp$ rt, referred to as $\Delta ku80$) [42]. Parasites were maintained in human
440 foreskin fibroblasts (HFF) with standard growth medium as previously described [43].

441 **Phylogenetic analysis**

442 The GSKs used in the phylogenetic analysis include TgGSK (EPT27729), PfGSK
443 (XP_001351197), AtBIN2 (Q39011), HsGSK3 α (P49840), and HsGSK3 β (P49841). Full
444 protein sequence alignment and phylogenetic analysis were performed using Clustal
445 Omega.

446 **Generation of parasite lines**

447 All primers used for molecular cloning are listed in supplemental table 1. To add a
448 hemagglutinin (HA) epitope tag to the endogenous TgGSK gene, we amplified the 3xHA-
449 DHFR [44] amplicon from the LIC-3xHA-DHFR plasmid using primers that allowed for
450 recombination at the 5' end with sequences immediately upstream of the stop codon and
451 at the 3' end with sequences after the Cas9 cutting site. To direct these templates to the
452 correct locus, we modified the plasmid pSag1-Cas9-U6-sgUPRT [45] using Q5 Site-
453 Directed Mutagenesis Kit (NEB) to replace the UPRT guide RNA sequence within the
454 plasmid to a guide RNA sequence of the target gene. The CRISPR/Cas9 plasmid and the
455 PCR amplicon were transfected into parental parasites using the Lonza Nucleofector and
456 the manufacturer's suggested protocols. Transfected parasites were selected using
457 pyrimethamine and cloned by limiting dilution as previously described [46].

458 To generate the TgGSK conditional knockdown strain, we utilized a CRISPR-Cas9
459 mediated strategy to introduce a tet-OFF cassette [47], which includes a transactivator
460 (TATi) protein, the drug-selective marker HXGPRT, and a tet response element (TRE)
461 followed by the Sag1 5' UTR, immediately upstream of the TgGSK gene start codon.
462 Specifically, a guide RNA targeting the TgGSK gene locus downstream of the start codon
463 was constructed by mutating the plasmid pSag1-Cas9-pU6-sgUPRT [45] using the Q5
464 mutagenesis kit. The tet-OFF cassette was amplified from the vector pT8TATi-HXGPRT-
465 tetO7S1 [47]. About 2 µg of the plasmid pSag1-Cas9-U6-sgGSK-KD and the PCR
466 amplicon from 200 µl of PCR reactions with 30 cycles were transfected into the TgGSK-
467 3xHA parasites using a Lonza nucleofector. Transfected parasites were then selected
468 with 50 mg/mL mycophenolic acid (MPS) and xanthine and cloned by limiting dilution.
469 Precise integration of the tet-OFF cassette was validated by PCR. The resulting strain
470 was designated as TATi-GSK.3xHA. To induce knockdown of GSK, this strain was grown
471 in 1µM of anhydrotetracycline (aTC) from Sigma Aldrich for the described length of time.

472 **Plaque assays**

473 Standard plaque assays were performed as previously described [43]. Briefly, 500
474 parasites of each strain were seeded into host cell monolayers grown in 12-well plates,
475 and cultures were then grown for six days. Cultures were then fixed with methanol and
476 stained with crystal violet. Host cell plaques were quantified as previously described [43].

477 **Immunofluorescence assays**

478 Immunofluorescence assays (IFAs) were performed as previously described [43]. The
479 primary antibodies used include rabbit anti-HA (Cell Signaling Technologies), rat anti-
480 IMC3 (provided by Dr. Marc-Jan Gubbels, Boston College), mouse anti-centrin 1 (Cell

481 Signaling Technologies), and mouse anti-acetylated tubulin (Sigma Aldrich) at a
482 concentration of 1:1000; guinea pig anti-TgEB1 (provided by Dr. Marc-Jan Gubbels,
483 Boston College) at a concentration of 1:3000; rabbit anti-TgH2Bz (provided by Dr. Laura
484 Vanagas and Dr. Sergio Angel, INTECH-Chascomus) at a concentration of 1:500; and
485 rabbit anti-Cpn60 (provided by Dr. Erica Dos Santos Martins, UFMG) at a concentration
486 of 1:300. Secondary antibodies used include Alexa Fluor 405, 488, 594, and 647
487 (Invitrogen) as well as DAPI (Thermo Fischer), all at 1:1000 or 1:2000. For images in
488 figures 2B and C, 3B, 4A, and 9A, a Nikon Eclipse E100080i microscope with NIS
489 Elements AR 3.0 software was used for imaging, followed by image analysis in ImageJ.
490 For images in figures 4D, 5A, and 6A, a Zeiss LSM800 confocal microscope with Zeiss
491 ZEN blue v2.0 and Huygens Professional v19.10.0p2 software was used for
492 deconvolution, followed by image analysis in ImageJ.

493 Quantification of the GSK-HA signal in the nucleus and cytoplasm was performed by
494 imaging 20 non-dividing vacuoles and 20 in late division using a Nikon Eclipse E100080i
495 microscope with NIS Elements AR 3.0 software. Using ImageJ, fluorescent intensity was
496 taken along a line in the cytosol and nucleus of a parasite in each vacuole before a ratio
497 of nuclear to cytosolic fluorescent intensity was calculated for each vacuole. Figure 2D
498 was made using GraphPad Prism software, and statistical analysis was performed using
499 a student's t-test.

500 **Ultrastructure expansion microscopy (UExM)**

501 Parasites were grown on HFF monolayers on round coverslips and then fixed for 20
502 minutes in 4% paraformaldehyde. Coverslips were then treated with a 1.4% formaldehyde
503 and 2% acrylamide solution in PBS overnight. Coverslips were inverted onto a solution of

504 5 μ L 10% APS, 5 μ L 10% TEMED, and 35 μ L monomer solution (21% sodium acrylate
505 solution, 28% acrylamide, 6% BIS, 11% 10x PBS) in a humid chamber and incubated on
506 ice for five minutes and then at 37°C for one hour. Each gel and coverslip were then put
507 in 2 mL of denaturation buffer (200 mM SDS, 200 mM NaCl, 50 mM Tris in water, pH 9)
508 on the rocker for 15 minutes to remove the gel from the coverslip. Each gel was then
509 placed in an Eppendorf tube with 1.5 mL of denaturation buffer and incubated at 95°C for
510 90 minutes. Each gel was then incubated three times in 25 mL of ddH₂O for 30 minutes
511 before being washed two times with 20 mL of 1x PBS for 15 minutes. Each gel was then
512 blocked for 30 minutes in 3% BSA/PBS before incubation overnight with 1 mL primary
513 antibody solution in 3% BSA/PBS at room temperature on the rocker. Gels were washed
514 three times with 2 mL PBS-T for 10 minutes before incubation with 1 mL secondary
515 antibody solution in PBS for 2.5 hours. Following another three PBS-T washes, gels were
516 incubated again three times in 25 mL ddH₂O for 30 minutes. Gels were then cut using the
517 opened top of a 15 mL falcon tube and placed in 35mm Cellvis coverslip bottomed dishes
518 that had been treated with poly-D-lysine. Primary antibodies used include rabbit anti-
519 *Toxoplasma* tubulin (provided by Dr. Michael Reese, UT Southwestern), rabbit anti-centrin
520 1, and mouse anti-HA at a concentration of 1:500. DRAQ5 (1:500) and NHS Ester (1:250)
521 were also used to visualize nuclear material and overall protein, respectively. Secondaries
522 used include Alexa Flour 488 and 594 at a concentration of 1:500. Imaging was performed
523 using a Zeiss LSM900 microscope with Zeiss ZEN Blue software before image analysis
524 using ImageJ.

525 **Western blots**

526 Western blots were performed as described previously [43]. The primary antibodies
527 used include rabbit anti-HA (Cell Signaling), mouse anti-Sag1 (Invitrogen), and mouse
528 anti-aldolase. The secondary antibodies utilized were HRP-labeled Anti-Mouse and Anti-
529 Rabbit IgG. The primary antibodies were used at a dilution of 1:5,000, while the secondary
530 antibodies were used at a dilution of 1:10,000. Imaging of the blot was performed using
531 a ProteinSimple system.

532 **Immunoprecipitation**

533 Immunoprecipitation was performed as previously described with some modifications
534 [46]. For immunoprecipitation from whole-parasite lysate, intracellular parasites of the
535 GSK.3xHA and Ku80 strains were grown for 18 hours in host cells. Parasites were
536 harvested with host cells by scraping in cold PBS and centrifugation at 2000 rcf for 5
537 minutes at 4°C. Cells were lysed with 500 µL RIPA lysis buffer supplemented with 5µL
538 protease and phosphatase inhibitor cocktail (Thermo Scientific) at 4°C for one hour. Each
539 sample was sonicated three times and centrifuged at maximum speed for 10 minutes at
540 4°C. The supernatant of each sample was incubated with mouse IgG magnetic beads for
541 one hour at 4°C for pre-cleaning. Samples were then incubated with rabbit HA magnetic
542 beads (Thermo Scientific) overnight at 4°C. After washing with RIPA lysis buffer and PBS,
543 the beads were submitted to the Indiana University School of Medicine Proteomics Core
544 facility for liquid chromatography coupled to tandem mass spectrometry (LC/MS-MS)
545 analysis.

546 **Global transcriptomic analysis**

547 TATi-GSK.3xHA parasites were grown for 18 hours with or without aTC in host cells.
548 Parasites were harvested with host cells by scraping in cold PBS, followed by
549 centrifugation at 2000 rcf for five minutes at 4°C. The pellet was passed through a syringe
550 in 10 mL PBS to release parasites from host cells, and the samples were centrifuged
551 again. The pellet was treated with 1 mL TRIZOL for five minutes at room temperature
552 before extracting RNA with 200 µL of chloroform and centrifuging at 12,000 rcf for 15
553 minutes at 4°C. The aqueous phase was again treated with 500 µL of chloroform and
554 centrifuged to extract as much RNA as possible. The aqueous phase was then mixed with
555 500 µL of isopropanol and incubated at room temperature for 10 minutes before
556 centrifuging at 12,000 rcf for 10 minutes. The RNA was washed with 1 mL 75% ethanol
557 and again centrifuged at 7,500 rcf for five minutes. The resulting RNA pellet was dried
558 and resuspended in 50 µL of nuclease-free water. Each condition was performed in
559 triplicate. Samples were stored at -80°C before being sent to AZENTA for library
560 construction and sequencing utilizing Illumina Next Generation Sequencing technology.
561 For each sample, ~30 M 2x150 bp pair-end reads were obtained. The GALAXY online
562 platform was used to perform data analysis. Specifically, the quality of the sequencing
563 data was checked using FastQC, and adapter sequences were trimmed using Trim
564 Galore. Hisat2 and htseq-count were separately employed to map reads to the genome
565 and count the reads of each transcript. DEseq2 was used to analyze differential gene
566 expression, and DEXseq was utilized to analyze whether the knockdown of TgGSK
567 affects alternative splicing. Pathway analysis was done through a combination of ToxoDB
568 and StringDB.

569 **Global phosphoproteomics**

570 TATi-GSK.3xHA parasites were grown for 24 hours with or without aTC in host cells.
571 Parasites were harvested via scraping in cold PBS and centrifuged at 2000 rcf for five
572 minutes at 4°C. Parasites were released from host cells using a syringe with a 27-gauge
573 needle, and the samples were centrifuged again. Each condition was performed in
574 triplicate. The parasite pellets were flash-frozen in liquid nitrogen and stored at -80°C
575 before being sent to the Indiana University School of Medicine Proteomics Core for global
576 phosphoproteome analysis, and they performed sample preparation and analysis as
577 described previously [6]. Protein function identification and pathway information were
578 determined using ToxoDB and StringDB.

579 **Garcinol assays**

580 GSK.3xHA parasites were seeded simultaneously with 2 or 4 µM Garcinol (BOC
581 Sciences) in 1% serum media for 18 hours. Immunofluorescence analysis and western
582 blots were done as described above.

583

584 **ACKNOWLEDGMENTS**

585 The mass spectrometry work was performed by the Indiana University School of
586 Medicine Center for Proteome Analysis. This research was supported by the National
587 Institutes of Health grants R01AI149766, R01DK124067, and R21AI164619 to G.A. The
588 Lab. of Apic. Biol. at Institut Pasteur de Montevideo is funded by a G4 grant awarded to
589 MEF by the Pasteur Network and FOCEM (MERCOSUR 645 Structural Convergence
590 Fund), COF 03/11. The authors gratefully acknowledge the Advanced Bioimaging Unit at
591 the Institut Pasteur Montevideo. MEF is a SNI and PEDECIBA researcher.

592

593

594 **REFERENCES**

- 595 1. Pappas G, Roussos N, Falagas ME. Toxoplasmosis snapshots: global status of
596 *Toxoplasma gondii* seroprevalence and implications for pregnancy and congenital
597 toxoplasmosis. *Int J Parasitol.* 2009;39: 1385–94. doi:10.1016/j.ijpara.2009.04.003
- 598 2. Luft B, Remington J. Toxoplasmic encephalitis in AIDS. *Clin Infect Dis.* 1992;15: 211–
599 222.
- 600 3. McAuley JB. Congenital Toxoplasmosis. *J Pediatr Infect Dis Soc.* 2014;3 Suppl 1:
601 S30-35. doi:10.1093/jpids/piu077
- 602 4. Black MW, Boothroyd JC. Lytic cycle of *Toxoplasma gondii*. *Microbiol Mol Biol Rev*
603 *MMBR.* 2000;64: 607–23.
- 604 5. Blader IJ, Coleman BI, Chen CT, Gubbels MJ. Lytic Cycle of *Toxoplasma gondii*: 15
605 Years Later. *Annu Rev Microbiol.* 2015;69: 463–85. doi:10.1146/annurev-micro-
606 091014-104100
- 607 6. Tomasina R, González FC, Francia ME. Structural and Functional Insights into the
608 Microtubule Organizing Centers of *Toxoplasma gondii* and *Plasmodium* spp.
609 *Microorganisms.* 2021;9: 2503. doi:10.3390/microorganisms9122503
- 610 7. Yang C, Doud EH, Sampson E, Arrizabalaga G. The protein phosphatase PPKL is a
611 key regulator of daughter parasite development in *Toxoplasma gondii*. *mBio.*
612 2023;14: e0225423. doi:10.1128/mbio.02254-23

- 613 8. Zhu J-Y, Sae-Seaw J, Wang Z-Y. Brassinosteroid signalling. *Dev Camb Engl.*
614 2013;140: 1615–1620. doi:10.1242/dev.060590
- 615 9. Kim T-W, Guan S, Sun Y, Deng Z, Tang W, Shang J-X, et al. Brassinosteroid signal
616 transduction from cell-surface receptor kinases to nuclear transcription factors. *Nat*
617 *Cell Biol.* 2009;11: 1254–1260. doi:10.1038/ncb1970
- 618 10. Qin CL, Tang J, Kim K. Cloning and in vitro expression of TPK3, a *Toxoplasma gondii*
619 homologue of shaggy/glycogen synthase kinase-3 kinases. *Mol Biochem Parasitol.*
620 1998;93: 273–283. doi:10.1016/s0166-6851(98)00042-5
- 621 11. Kannan N, Neuwald AF. Evolutionary constraints associated with functional
622 specificity of the CMGC protein kinases MAPK, CDK, GSK, SRPK, DYRK, and
623 CK2alpha. *Protein Sci Publ Protein Soc.* 2004;13: 2059–2077.
624 doi:10.1110/ps.04637904
- 625 12. Treeck M, Sanders JL, Elias JE, Boothroyd JC. The phosphoproteomes of
626 *Plasmodium falciparum* and *Toxoplasma gondii* reveal unusual adaptations within
627 and beyond the parasites' boundaries. *Cell Host Microbe.* 2011;10: 410–9.
628 doi:10.1016/j.chom.2011.09.004
- 629 13. Sidik SM, Huet D, Ganesan SM, Huynh M-H, Wang T, Nasamu AS, et al. A Genome-
630 Wide CRISPR Screen in *Toxoplasma* Identifies Essential Apicomplexan Genes. *Cell.*
631 2016;166: 1423-1435.e12. doi:10.1016/j.cell.2016.08.019

- 632 14. Meissner M, Brecht S. Modulation of myosin A expression by a newly established
633 tetracycline repressor-based inducible system in *Toxoplasma gondii*. *Nucleic Acids*
634 *Res.* 2001;29: E115–E115.
- 635 15. Striepen B, Crawford MJ, Shaw MK, Tilney LG, Seeber F, Roos DS. The plastid of
636 *Toxoplasma gondii* is divided by association with the centrosomes. *J Cell Biol.*
637 2000;151: 1423–1434. doi:10.1083/jcb.151.7.1423
- 638 16. Fiol CJ, Mahrenholz AM, Wang Y, Roeske RW, Roach PJ. Formation of protein
639 kinase recognition sites by covalent modification of the substrate. Molecular
640 mechanism for the synergistic action of casein kinase II and glycogen synthase
641 kinase 3. *J Biol Chem.* 1987;262: 14042–14048.
- 642 17. Wang J, Dixon SE, Ting LM, Liu TK, Jeffers V, Croken MM, et al. Lysine
643 Acetyltransferase GCN5b Interacts with AP2 Factors and Is Required for
644 *Toxoplasma gondii* Proliferation. *PLoS Pathog.* 2014;10: e1003830.
645 doi:10.1371/journal.ppat.1003830
- 646 18. Jeffers V, Gao H, Checkley LA, Liu Y, Ferdig MT, Sullivan WJ. Garcinol Inhibits
647 GCN5-Mediated Lysine Acetyltransferase Activity and Prevents Replication of the
648 Parasite *Toxoplasma gondii*. *Antimicrob Agents Chemother.* 2016;60: 2164–2170.
649 doi:10.1128/AAC.03059-15
- 650 19. Saidi Y, Hearn TJ, Coates JC. Function and evolution of “green” GSK3/Shaggy-like
651 kinases. *Trends Plant Sci.* 2012;17: 39–46. doi:10.1016/j.tplants.2011.10.002

- 652 20. Kaidanovich-Beilin O, Woodgett JR. GSK-3: Functional Insights from Cell Biology
653 and Animal Models. *Front Mol Neurosci.* 2011;4: 40. doi:10.3389/fnmol.2011.00040
- 654 21. Jonak C, Hirt H. Glycogen synthase kinase 3/SHAGGY-like kinases in plants: an
655 emerging family with novel functions. *Trends Plant Sci.* 2002;7: 457–461.
656 doi:10.1016/s1360-1385(02)02331-2
- 657 22. Hughes K, Nikolakaki E, Plyte SE, Totty NF, Woodgett JR. Modulation of the
658 glycogen synthase kinase-3 family by tyrosine phosphorylation. *EMBO J.* 1993;12:
659 803–808. doi:10.1002/j.1460-2075.1993.tb05715.x
- 660 23. Mao J, Li J. Regulation of Three Key Kinases of Brassinosteroid Signaling Pathway.
661 *Int J Mol Sci.* 2020;21. doi:10.3390/ijms21124340
- 662 24. Monteserin-Garcia J, Al-Massadi O, Seoane LM, Alvarez CV, Shan B, Stalla J, et al.
663 Sirt1 inhibits the transcription factor CREB to regulate pituitary growth hormone
664 synthesis. *FASEB J Off Publ Fed Am Soc Exp Biol.* 2013;27: 1561–1571.
665 doi:10.1096/fj.12-220129
- 666 25. Morlon-Guyot J, Francia ME, Dubremetz J-F, Daher W. Towards a molecular
667 architecture of the centrosome in *Toxoplasma gondii*. *Cytoskelet Hoboken NJ.*
668 2017;74: 55–71. doi:10.1002/cm.21353
- 669 26. Leung JM, Liu J, Wetzel LA, Hu K. Centrin2 from the human parasite *Toxoplasma*
670 *gondii* is required for its invasion and intracellular replication. *J Cell Sci.* 2019;132:
671 jcs228791. doi:10.1242/jcs.228791

- 672 27. Yoshino Y, Ishioka C. Inhibition of glycogen synthase kinase-3 beta induces
673 apoptosis and mitotic catastrophe by disrupting centrosome regulation in cancer
674 cells. *Sci Rep.* 2015;5: 13249. doi:10.1038/srep13249
- 675 28. Fumoto K, Hoogenraad CC, Kikuchi A. GSK-3beta-regulated interaction of BICD with
676 dynein is involved in microtubule anchorage at centrosome. *EMBO J.* 2006;25:
677 5670–5682. doi:10.1038/sj.emboj.7601459
- 678 29. Shinde MY, Sidoli S, Kulej K, Mallory MJ, Radens CM, Reicherter AL, et al.
679 Phosphoproteomics reveals that glycogen synthase kinase-3 phosphorylates
680 multiple splicing factors and is associated with alternative splicing. *J Biol Chem.*
681 2017;292: 18240–18255. doi:10.1074/jbc.M117.813527
- 682 30. Heyd F, Lynch KW. Phosphorylation-dependent regulation of PSF by GSK3 controls
683 CD45 alternative splicing. *Mol Cell.* 2010;40: 126–137.
684 doi:10.1016/j.molcel.2010.09.013
- 685 31. Kim T-W, Park CH, Hsu C-C, Kim Y-W, Ko Y-W, Zhang Z, et al. Mapping the signaling
686 network of BIN2 kinase using TurboID-mediated biotin labeling and
687 phosphoproteomics. *Plant Cell.* 2023;35: 975–993. doi:10.1093/plcell/koad013
- 688 32. Harris MT, Jeffers V, Martynowicz J, True JD, Mosley AL, Sullivan WJ. A novel
689 GCN5b lysine acetyltransferase complex associates with distinct transcription
690 factors in the protozoan parasite *Toxoplasma gondii*. *Mol Biochem Parasitol.*
691 2019;232: 111203. doi:10.1016/j.molbiopara.2019.111203

- 692 33. Narita T, Weinert BT, Choudhary C. Functions and mechanisms of non-histone
693 protein acetylation. *Nat Rev Mol Cell Biol.* 2019;20: 156–174. doi:10.1038/s41580-
694 018-0081-3
- 695 34. Glozak MA, Sengupta N, Zhang X, Seto E. Acetylation and deacetylation of non-
696 histone proteins. *Gene.* 2005;363: 15–23. doi:10.1016/j.gene.2005.09.010
- 697 35. Choudhary C, Kumar C, Gnad F. Lysine acetylation targets protein complexes and
698 co-regulates major cellular functions. *Science.* 2009;325: 834–840.
- 699 36. Silmon de Monerri NC, Yakubu RR, Chen AL, Bradley PJ, Nieves E, Weiss LM, et
700 al. The Ubiquitin Proteome of *Toxoplasma gondii* Reveals Roles for Protein
701 Ubiquitination in Cell-Cycle Transitions. *Cell Host Microbe.* 2015;18: 621–633.
702 doi:10.1016/j.chom.2015.10.014
- 703 37. Caron C, Boyault C, Khochbin S. Regulatory cross-talk between lysine acetylation
704 and ubiquitination: role in the control of protein stability. *BioEssays News Rev Mol*
705 *Cell Dev Biol.* 2005;27: 408–415. doi:10.1002/bies.20210
- 706 38. Sarikhani M, Mishra S, Maity S, Kotyada C, Wolfgeher D, Gupta MP, et al. SIRT2
707 deacetylase regulates the activity of GSK3 isoforms independent of inhibitory
708 phosphorylation. *eLife.* 2018;7: e32952. doi:10.7554/eLife.32952
- 709 39. Zhou Q, Li S, Li M, Ke D, Wang Q, Yang Y, et al. Human tau accumulation promotes
710 glycogen synthase kinase-3 β acetylation and thus upregulates the kinase: A vicious
711 cycle in Alzheimer neurodegeneration. *EBioMedicine.* 2022;78: 103970.
712 doi:10.1016/j.ebiom.2022.103970

- 713 40. Hao Y, Wang H, Qiao S, Leng L, Wang X. Histone deacetylase HDA6 enhances
714 brassinosteroid signaling by inhibiting the BIN2 kinase. *Proc Natl Acad Sci U S A.*
715 2016;113: 10418–10423. doi:10.1073/pnas.1521363113
- 716 41. Jeffers V, Sullivan WJ Jr. Lysine Acetylation Is Widespread on Proteins of Diverse
717 Function and Localization in the Protozoan Parasite *Toxoplasma gondii*. *Eukaryot*
718 *Cell.* 2012;11: 735–42. doi:10.1128/EC.00088-12
- 719 42. Huynh M, Carruthers V. Tagging of endogenous genes in a *Toxoplasma gondii* strain
720 lacking Ku80. *Eukaryot Cell.* 2009;8: 530–539. doi:10.1128/EC.00358-08
- 721 43. Yang C, Broncel M, Dominicus C, Sampson E, Blakely WJ, Treeck M, et al. A plasma
722 membrane localized protein phosphatase in *Toxoplasma gondii*, PPM5C, regulates
723 attachment to host cells. *Sci Rep.* 2019;9: 5924. doi:10.1038/s41598-019-42441-1
- 724 44. Garrison E, Treeck M, Ehret E, Butz H, Garbuz T, Oswald BP, et al. A Forward
725 Genetic Screen Reveals that Calcium-dependent Protein Kinase 3 Regulates Egress
726 in *Toxoplasma*. Soldati-Favre D, editor. *PLoS Pathog.* 2012;8: e1003049–e1003049.
727 doi:10.1371/journal.ppat.1003049
- 728 45. Brown KM, Long S, Sibley LD. Conditional Knockdown of Proteins Using Auxin-
729 inducible Degron (AID) Fusions in *Toxoplasma gondii*. *Bio-Protoc.* 2018;8.
730 doi:10.21769/BioProtoc.2728
- 731 46. Yang C, Blakely WJ, Arrizabalaga G. The Tyrosine Phosphatase PRL Regulates
732 Attachment of *Toxoplasma gondii* to Host Cells and Is Essential for Virulence.
733 *mSphere.* 2022;7: e0005222. doi:10.1128/msphere.00052-22

734 47. Salamun J, Kallio JP, Daher W, Soldati-Favre D, Kursula I. Structure of *Toxoplasma*
735 *gondii* coronin, an actin-binding protein that relocalizes to the posterior pole of
736 invasive parasites and contributes to invasion and egress. *FASEB J.* 2014 [cited 11
737 Feb 2019]. doi:10.1096/fj.14-252569

738

739

740

ID number	Protein annotation
TgGT1_214960	AP2X-8
TgGT1_217050	ADA2a
TgGT1_226620	Hypothetical protein
TgGT1_229640	Hypothetical protein
TgGT1_241850	Hypothetical protein
TgGT1_243440	GCN5b
TgGT1_274180	Hypothetical protein
TgGT1_280590	Hypothetical protein
TgGT1_290630	AP2IX-7

741

742 **Table 1. TgGSK interactors.** ID number and annotation of putative interactors of TgGSK
743 identified in both IPs performed with a ratio of experimental over control higher than 5.
744 Members of the GCN5b complex are shown in grey.

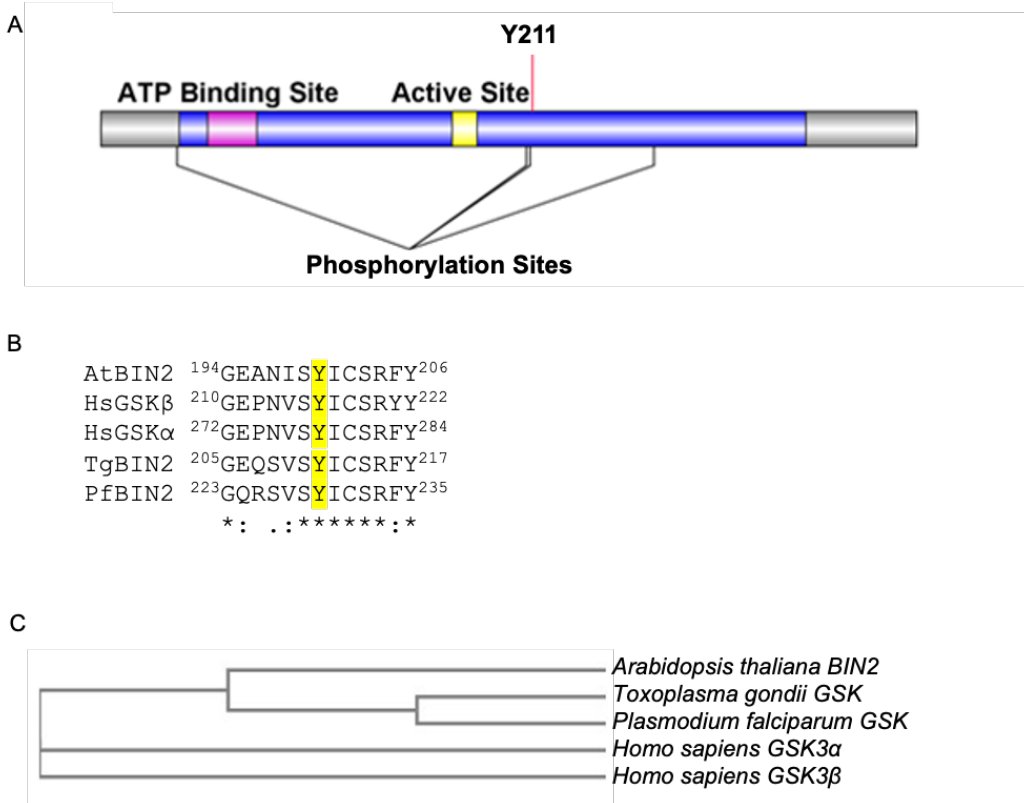


Figure 1. TgGSK is closely related to plant BIN2. A. Graphical representation of the TgGSK protein, with the relative position of the catalytic domain (blue), ATP binding site (magenta), and active site (yellow). Conserved acetylation (K76) and phosphorylation (Y211) sites are shown. B. Alignment of regions containing the conserved lysine and tyrosine from GSKs from *Arabidopsis thaliana* (Q39011), *Homo sapiens* (P49841, P49840), *Toxoplasma gondii* (EPT27729), and *Plasmodium falciparum* (XP_001351197) performed by Clustal Omega. C. Phylogenetic analysis of GSKs derived from Clustal Omega alignment.

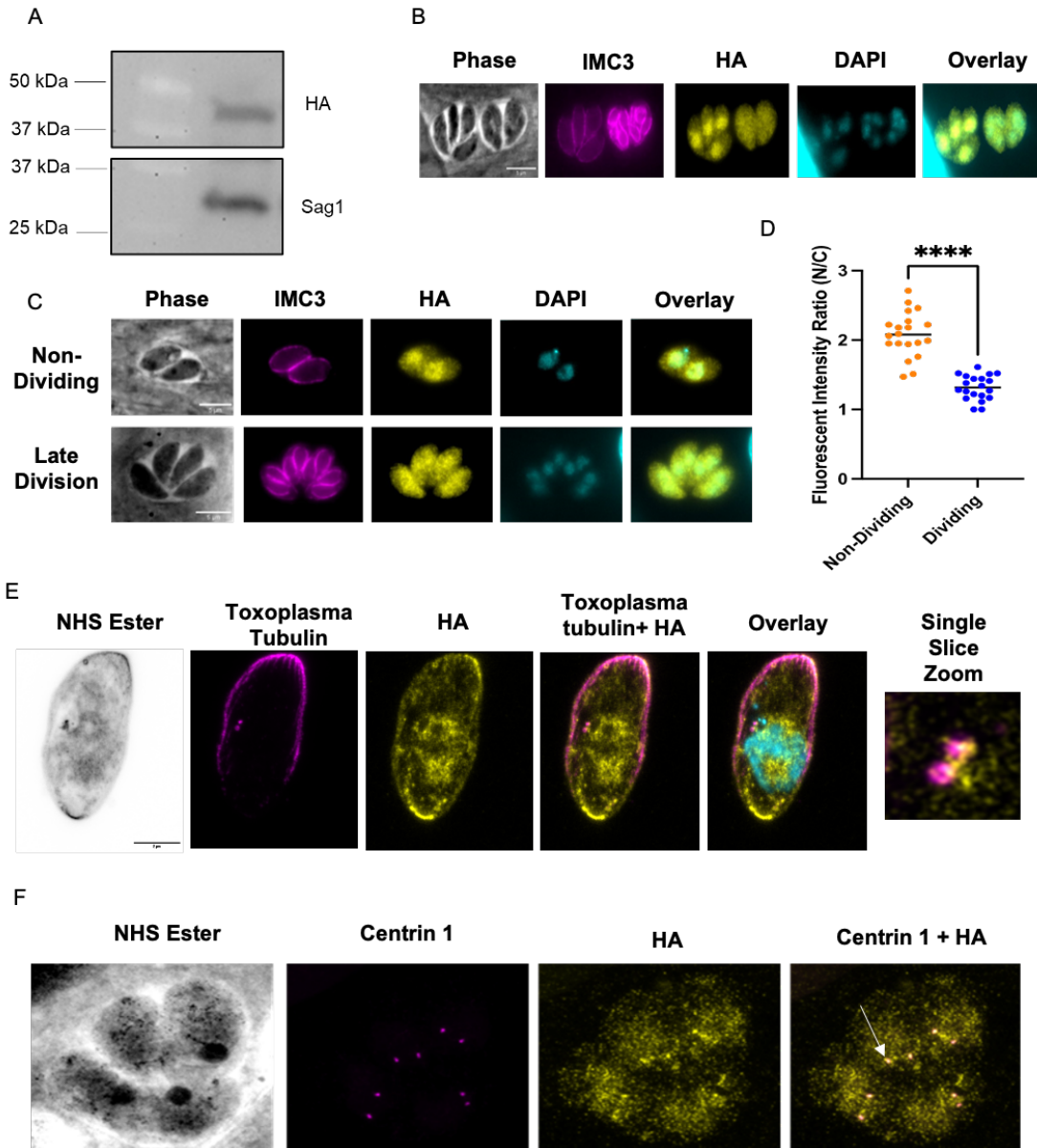


Figure 2. TgGSK has a dynamic, cell cycle-dependent localization. A. Western blot of protein extract from parasites in which the endogenous TgGSK includes a 3xHA epitope tag. Blots were stained for HA (top) and Sag 1 (bottom). B and C. Parasites of the TgGSK.3xHA strain were grown intracellularly for 24 hours before performing IFA using antibodies against HA and IMC3, and the DNA stain DAPI. In C, parasites in the top panels are not dividing, while those in the bottom panel are undergoing division. D.

Quantification of the fluorescent intensity ratio of nucleus to cytosol in non-dividing and dividing parasites; n=20 per condition, p<0.0005. E. Expansion microscopy of a non-dividing parasite staining for *Toxoplasma* tubulin (magenta), HA (yellow), and DRAQ5 (cyan, color in overlay) to visualize parasite structure and centrosomes, TgGSK, and nuclear material, respectively. A single slice zoomed image of the centrosomes is shown to closer visualize TgGSK localization to this organelle. F. Expansion microscopy of four dividing parasites in a vacuole staining for Centrin 1 and HA to visualize TgGSK's colocalization with the centrosomes. Arrowhead shows an example of TgGSK colocalized with a centrosome.

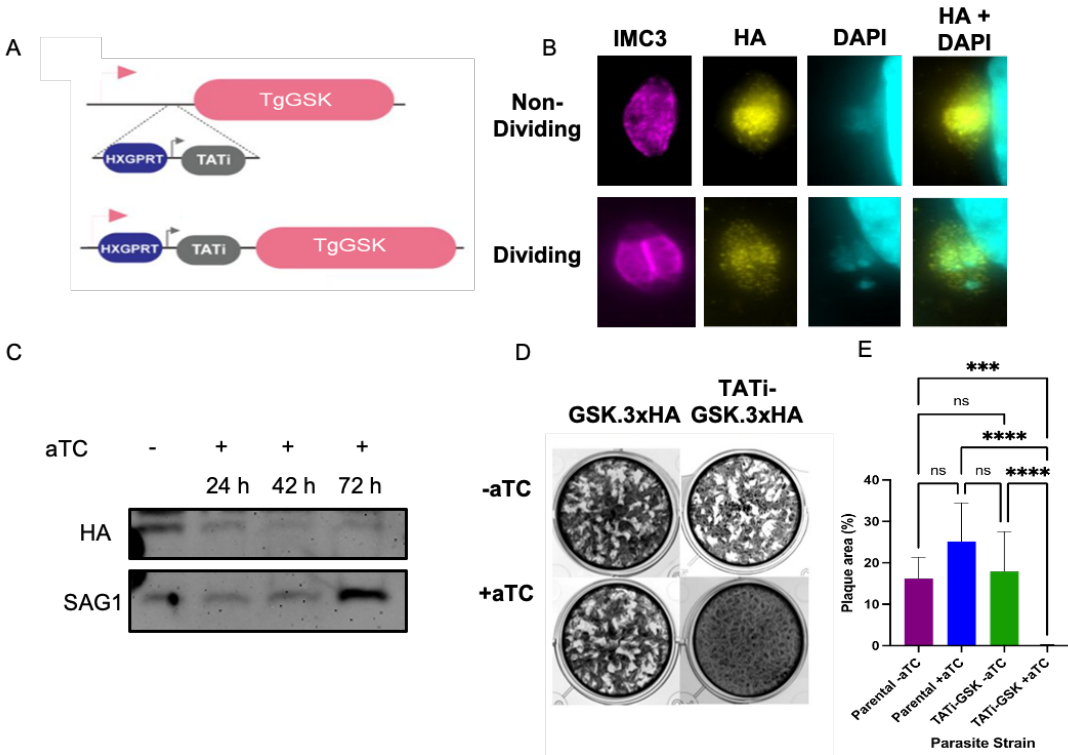


Figure 3. TgGSK is essential for propagation in tissue culture. A. Graphical representation of the strategy used to engineer a TgGSK conditional knockdown strain using the TATi tetracycline regulatable system. B. Parasites of the TATi-GSK.3xHA strain were grown in culture for 24 hours to perform IFA with antibodies against IMC3 and HA and the DNA stain DAPI without the addition of aTC. C. Western blot of protein extract from TATi-GSK.3xHA parasites grown in no aTC (-) or in aTC for 24, 42, or 72 hours. Blots were probed for HA to monitor TgGSK or Sag1 as loading control. D. Plaque assay of parental (GSK.3xHA) and TATi-GSK.3xHA knockdown parasites incubated for 6 days with or without aTC. E. Quantification of plaque assay. ****: $p < 0.0005$, ***: $p < 0.005$, ns: no significance, $n = 9$ wells per condition (3 biological replicates with 3 experimental replicates each).

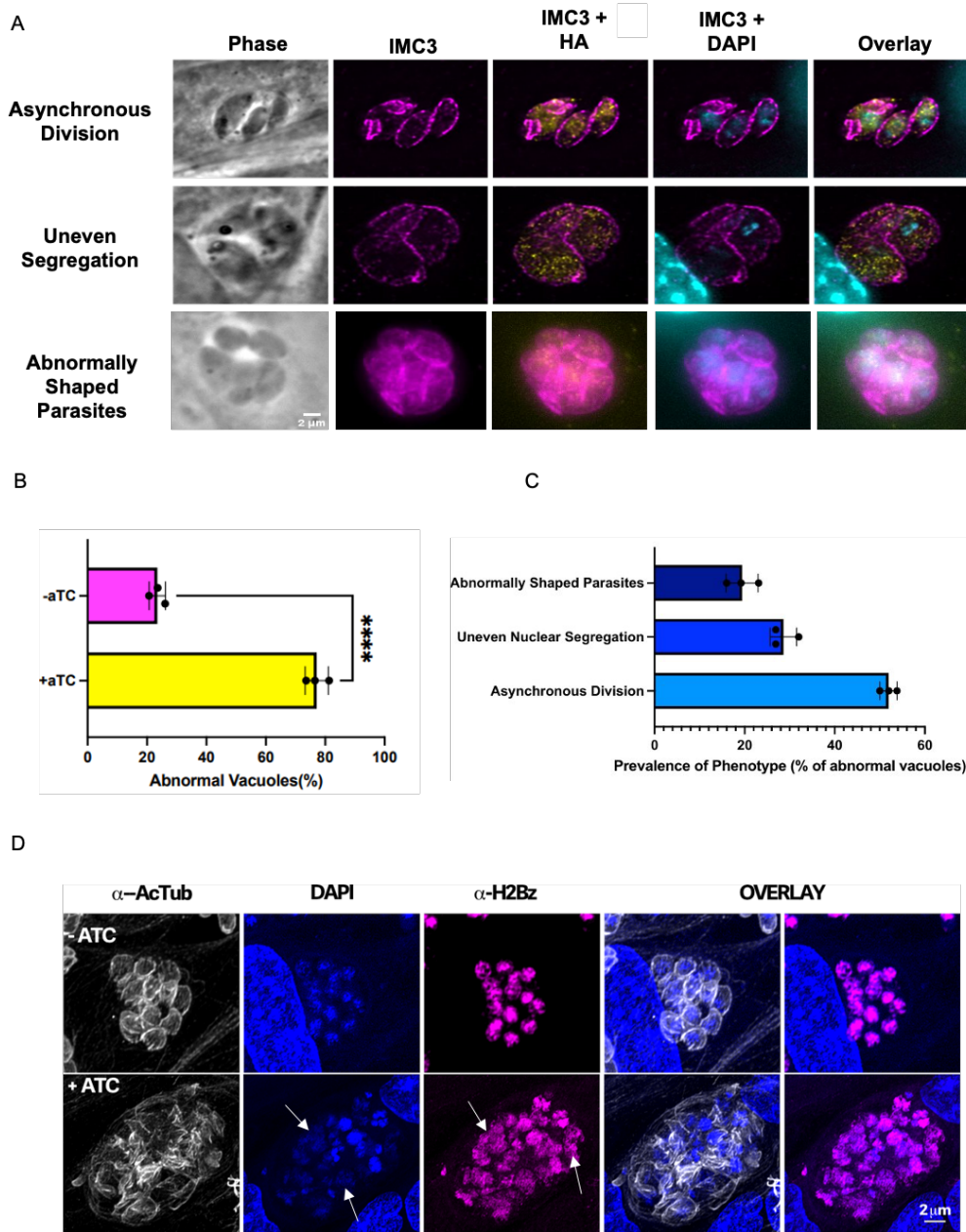


Figure 4. Knockdown of TgGSK causes abnormal division phenotypes. A. IFA of TgGSK knockdown parasites after 42 hours of incubation with aTC. IMC3, HA, and DAPI staining visualize mother and daughter cell IMC, TgGSK, and nuclear material, respectively. Representatives of the main phenotypes observed are shown B. Quantification of the percentage of normal vacuoles in TATI-GSK parasites with and without 42-hour incubation with aTC. N= 3, 100 total parasites over the replicates. The

error percentage shown is the standard deviation. C. Quantification of the different division phenotypes seen after 42 hours of TgGSK knockdown. D. IFA showing division phenotypes of TgGSK knockdown parasites after 96 hours of incubation with aTC. Acetylated tubulin, DAPI, and H2Bz staining visualize parasite structure, nuclear material, and histones, respectively. Arrowheads point to diffuse nuclear material and H2 histone.

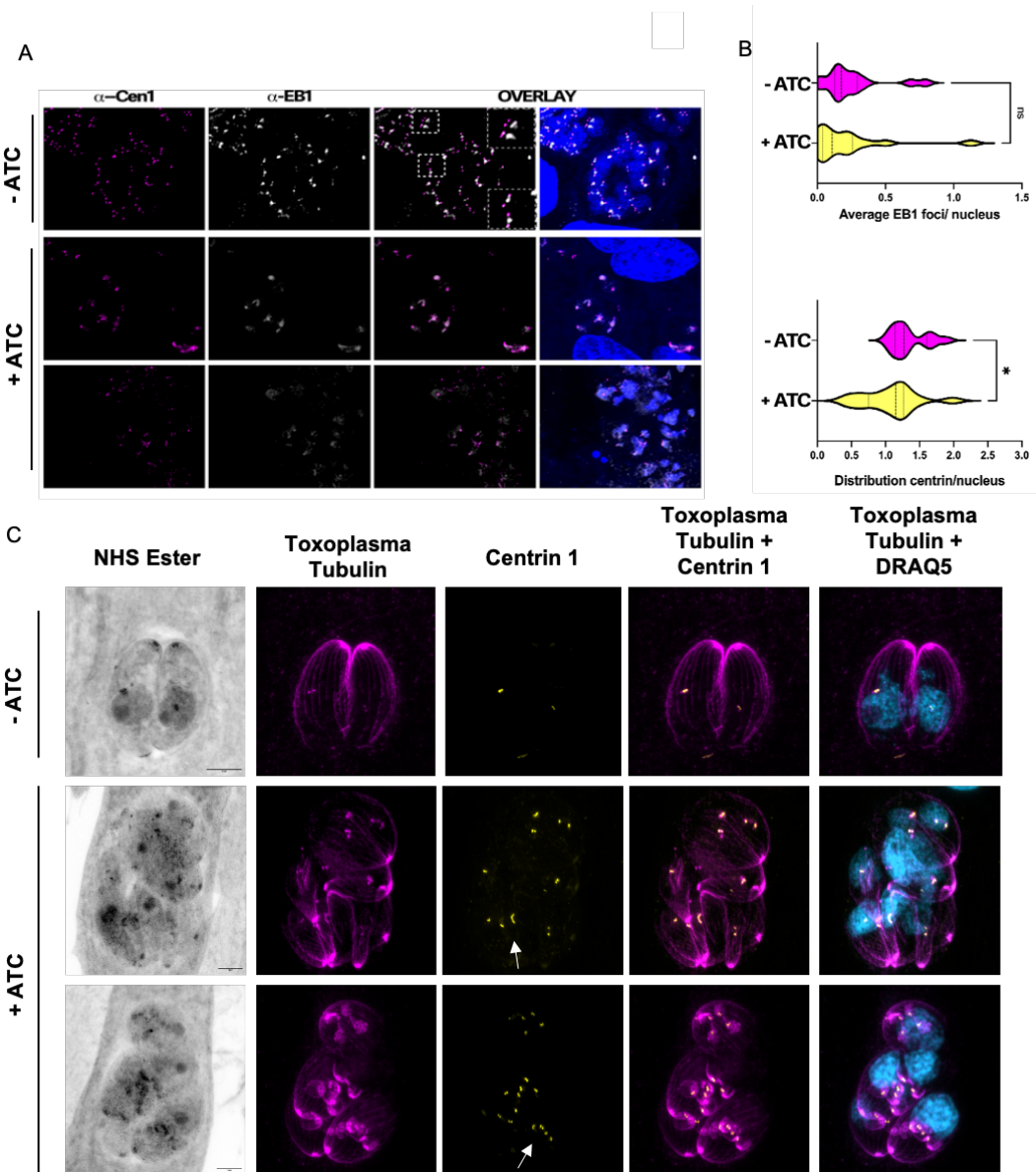


Figure 5. TgGSK knockdown parasites have a centrosome duplication defect. A. IFA TATI-GSK parasites treated with aTC for 96 hours stained for centrin 1 (centrosomes) and EB1 mitotic spindles). Outlined boxes show parasites with abnormally dividing centrosomes. **B.** Quantification of centrin and EB1 signal in (A) measuring distribution of signal per parasite nucleus. N= 3 replicates with 100 vacuoles quantified. Statistical analysis: two-tailed t-test with Welch's correction. *: p<0.05 ns: no significance. **C.**

Expansion microscopy of TATi-GSK parasites treated with aTC for 42 hours. Arrows indicate elongated centrosomes that seem unable to undergo fission.

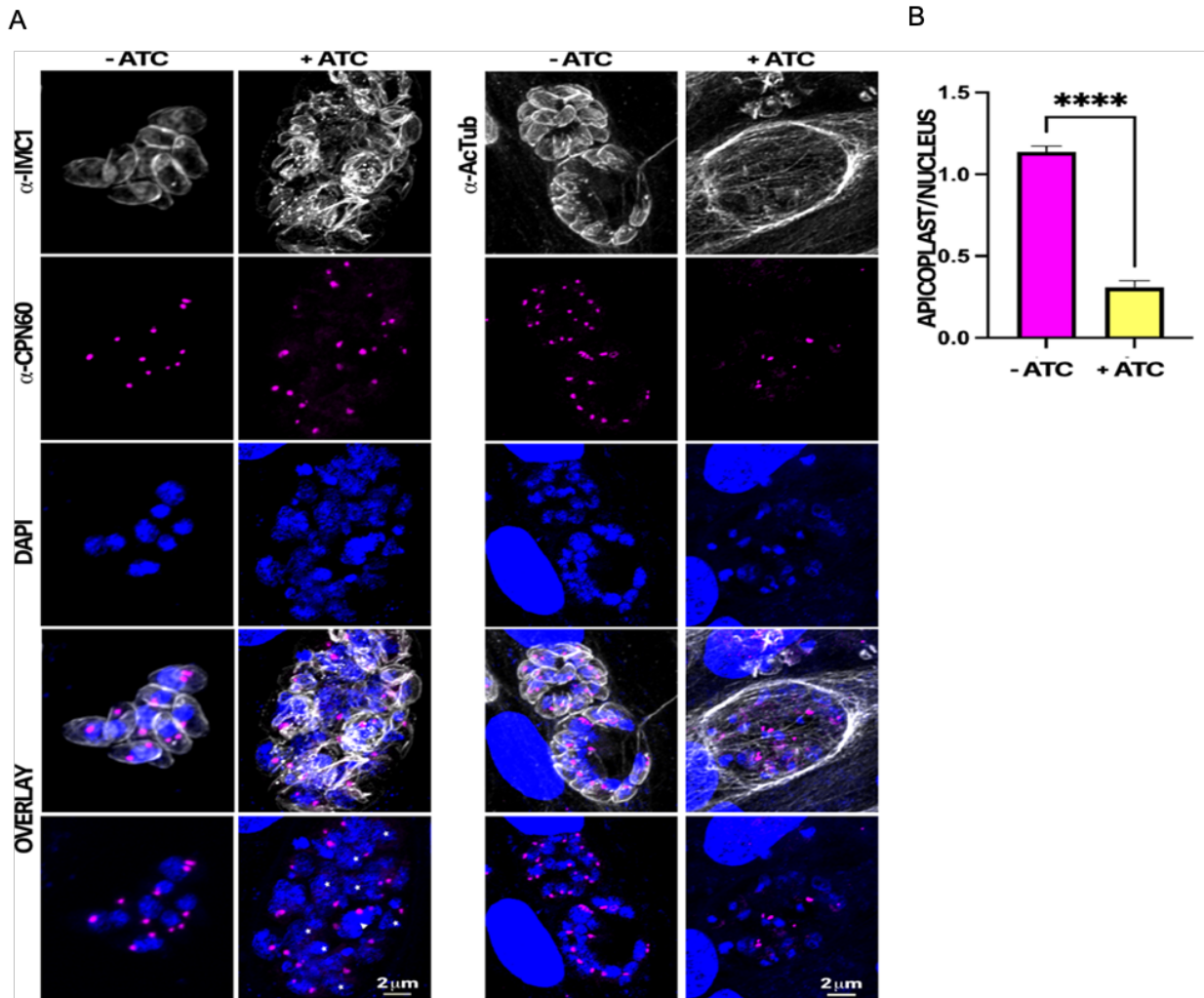


Figure 6. TgGSK knockdown parasites display a reduction in apicoplast material.

A. IFA of TATI-GSK parasites after 96 hours of aTC treatment stained for the apicoplast marker CPN60. IMC1 and DAPI staining are also used to visualize parasite structure and nuclear material. B. Quantification of the number of apicoplast foci per parasite nucleus in TgGSK knockdown versus control parasites. ****: p<0.0005 n=3 experimental replicates, 100 total parasites quantified.

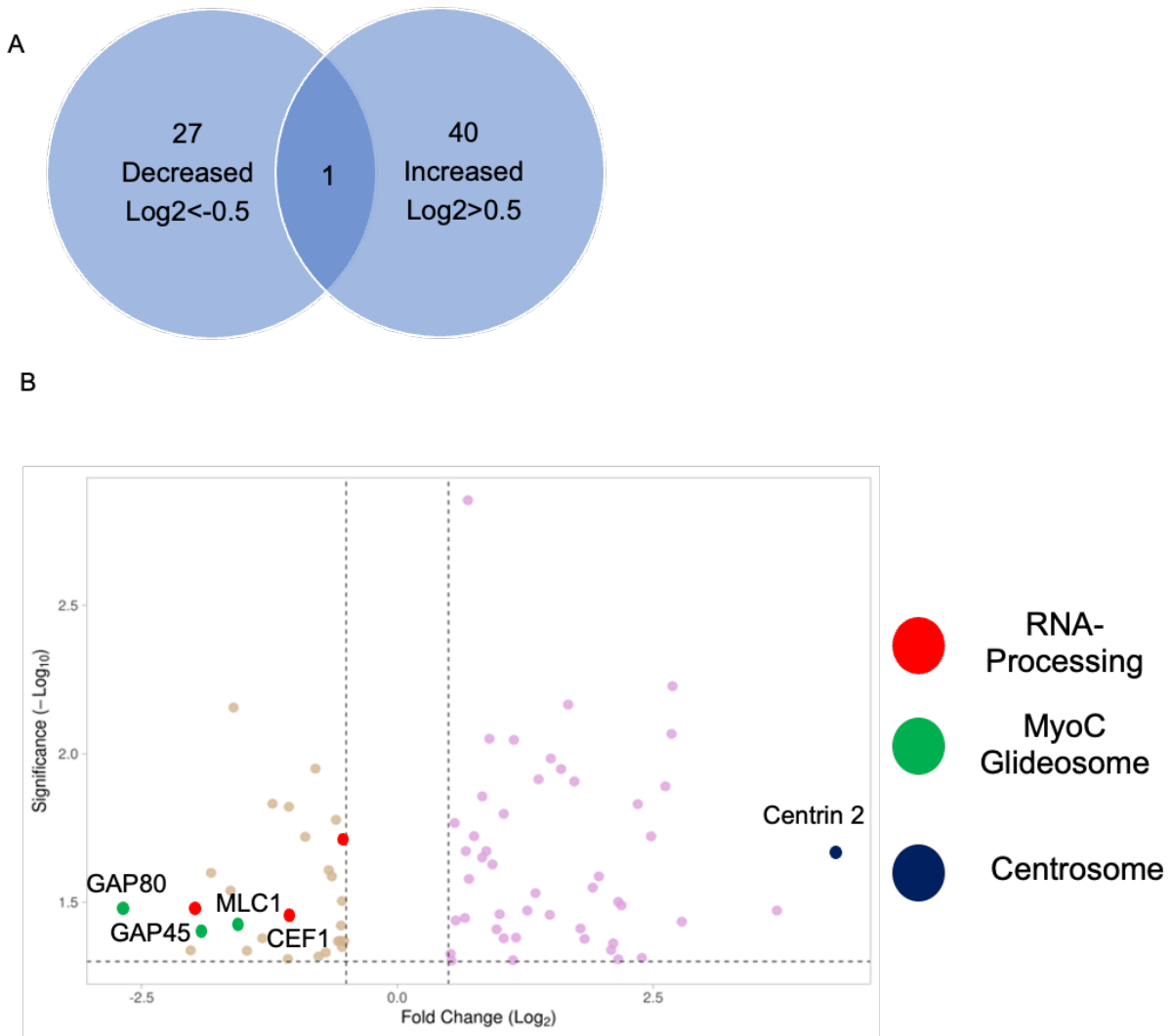


Figure 7. Global Phosphoproteome analysis reveals TgGSK-dependent phosphorylation events. A. Number of proteins that had increased or decreased phosphorylation after 24 hours of TgGSK knockdown. One protein had peptides with both increased and decreased phosphorylation. B. Volcano plot of all differentially phosphorylated proteins with a log₂fold change >0.5 and p<0.05. Splicing, myoC glideosome, and centrosome proteins are highlighted.

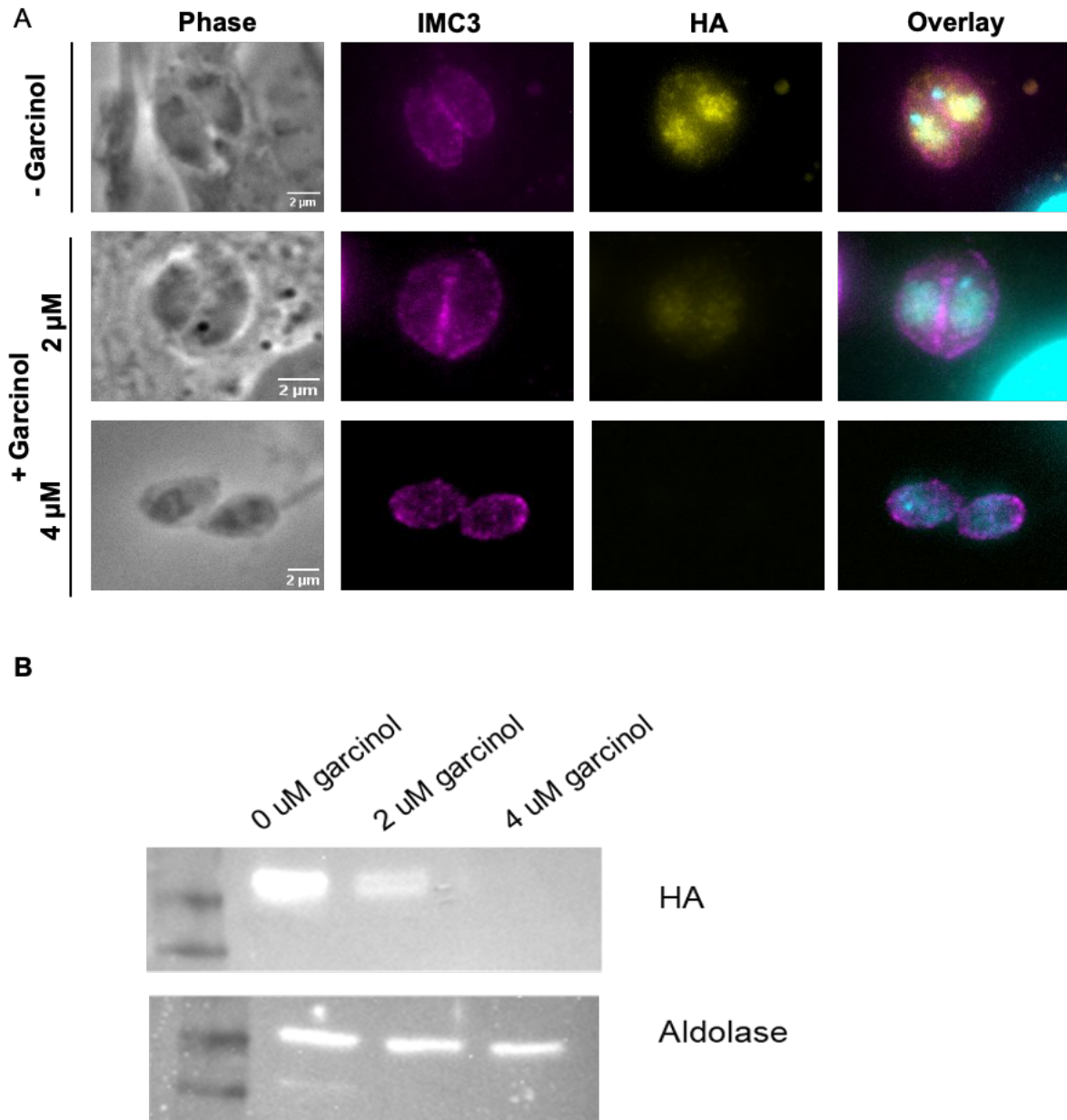


Figure 8. Acetylation by GCN5b stabilizes TgGSK. A. IFA of non-dividing GSK.3xHA parasites treated with 0, 2, or 4 μ M Garcinol for 18 hours. Staining was done for IMC3, HA, and DAPI to visualize IMC, TgGSK, and nuclear material, respectively. B. Western blot analysis of TgGSK protein levels after 18 hours of Garcinol treatment. The cytosolic protein aldolase was used as a control.

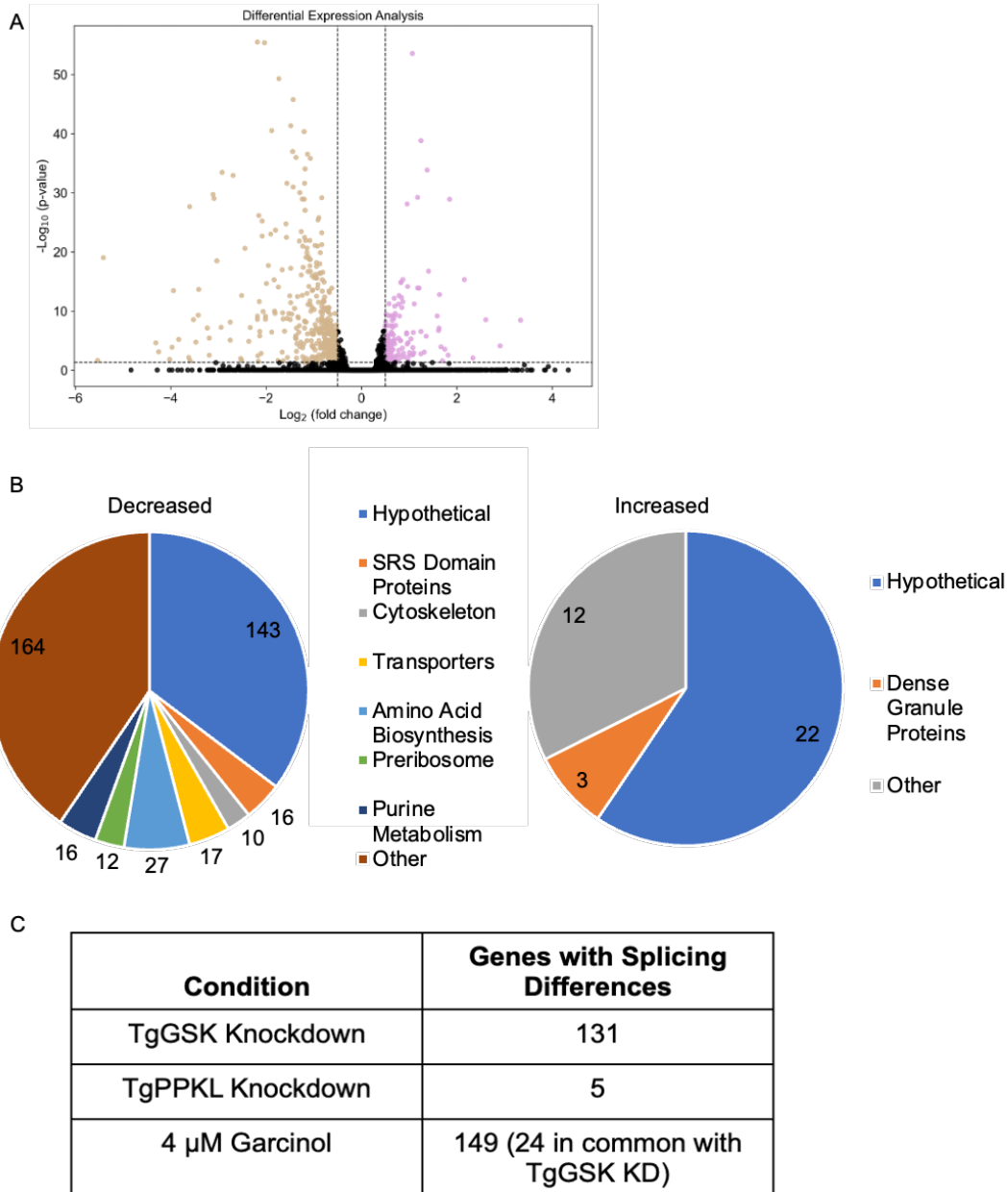


Figure 9. Global transcriptome analysis of TgGSK knockdown parasites. A. Volcano plot showing all differentially transcribed genes with a log2fold change >0.5 and $p < 0.05$ after 18 hours of TgGSK knockdown. B. Biological processes with enriched transcriptome changes as identified by ToxoDB and StringDB. C. Genes that were differentially spliced after TgGSK knockdown, TgPPKL knockdown, and treatment with 4 μ M Garcinol.

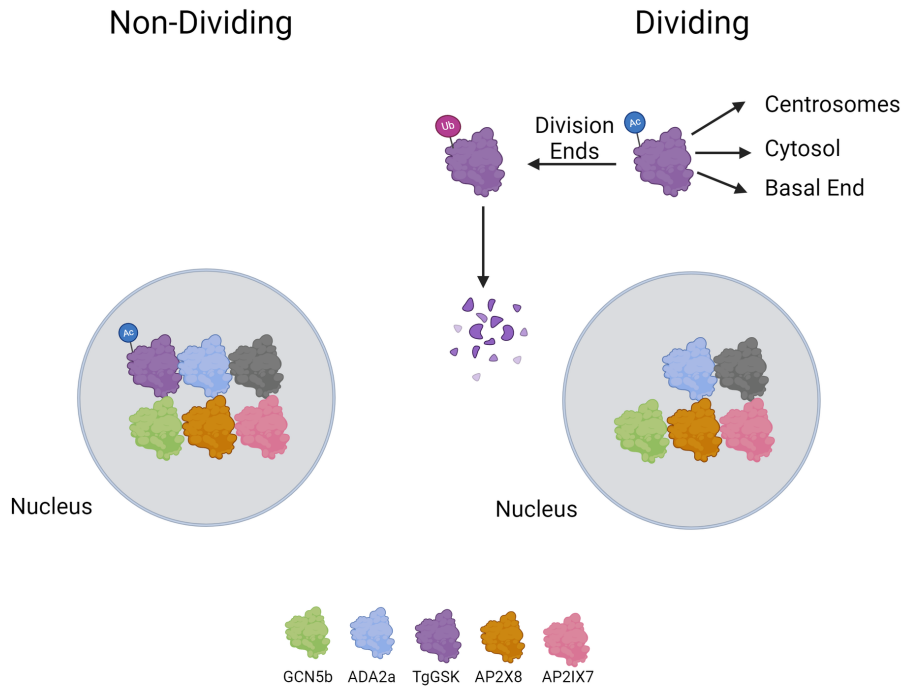
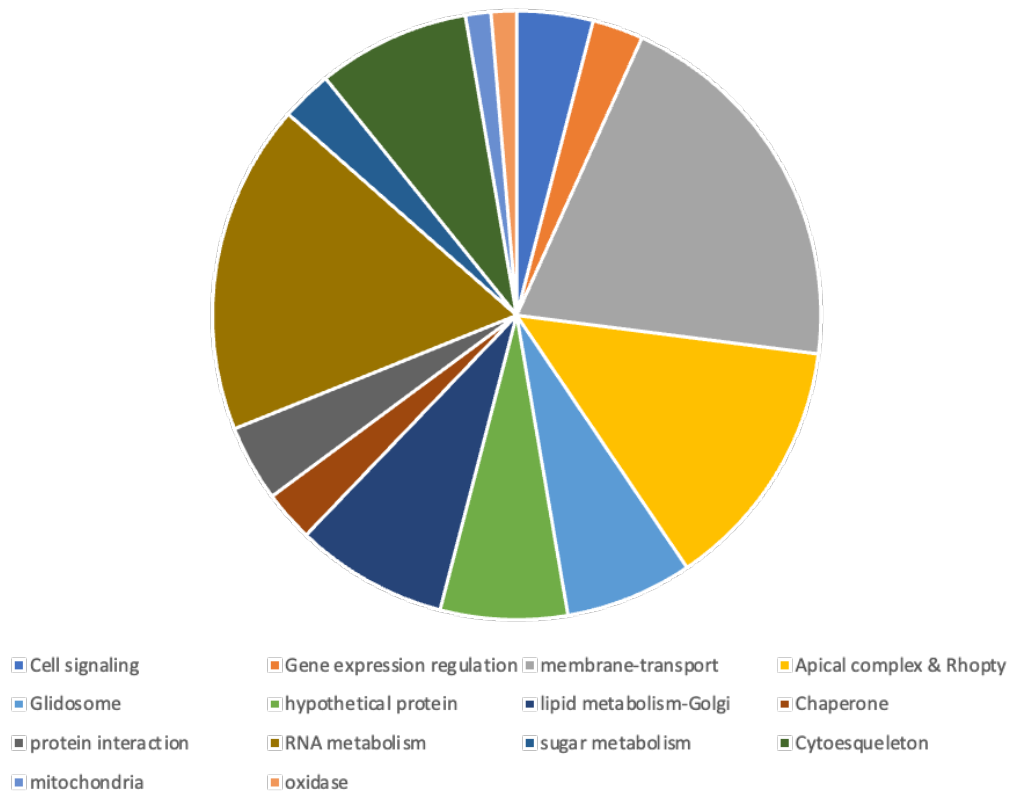


Figure 10. Model of the regulation and function of TgGSK. A preliminary model of TgGSK in non-dividing and dividing parasites. Image created using Biorender.

Purpose	Name	Sequence
Generate pSag1-Cas9-U6-sgGSK-TG-HXG CRSPR/Cas9 plasmid for endogeneous tagging	GSK-tg-sgRNA.For	GTCTTTTTTTGTTTTAGAGCTAGAAATAGC
	GSK-tg-sgRNA.Rev	CGACAGCTGCAACTTGACATCCCCATTTAC
Amplify 3xHA-DHFR cassette from the plasmid pLIC-3xHA-DHFR	GSK-TG-insert.For	ATGTATTCCGAAGCATATCGCCAGTGCAAACAACC GTGGCTTAATTAATAATTGGAAGTGGAGG
	GSK-TG-insert.Rev	AGCATAAGAGAAGCTCCCCATCCCTAGTAGGTGTA GGGAGGTTTTCCAGTCACGACG
Generate pSag1-Cas9-U6-sgGSK-TATI-HXG CRSPR/Cas9 plasmid for endogeneous tagging	GSK-TATI-sgRNA.For	AAGAAGGGGTGTTTTAGAGCTAGAAATAGC
	GSK-TATI-sgRNA.Rev	TCCTTCGTCCAAGTTGACATCCCCATTTAC
Amplify TATi cassette from the plasmid 5'COR-pT8TATi1-HX-tetO7S1mycNtCOR.dna	GSK-TATI-insert.For	CACTCATCTTTTCTGGCCTTTGTCGAGAAGGCAG AAGTCTTCTCATGTTTGCGGATCCG
	GSK-TATI-insert.Rev	CTACTCTTCTGAGCAGCTGCGGGATCGTACTGCG GGTCCGGCATTGATATCCCTAGGAATCACTC

Supplemental table 1. Primers used in this work. Sequences are 5' to 3'.



Supplemental figure S1. Classification of hypothetical proteins with TgGSK-dependent phosphopeptides. Hypothetical proteins with peptides differentially phosphorylated in the knockdown vs the parental were analyzed based on annotations in the *Toxoplasma* genome database or homology to proteins in other Apicomplexan species. Additionally, the protein domains were analyzed based on known conserved functions. Some of these proteins remained classified as hypothetical.